Stabilized Capacity Analysis for Steel Tube Confined Concrete Columns

Yongjian Chen[1], Jia Tina Du[2]

1. PhD Candidate, School of Civil, Environmental and Mining Engineering, University of Adelaide, SA 5005, Australia. Email:yongjian.chen@adelaide.edu.au

2. School of Computer and Information Science, University of South Australia, SA 5001, Australia. Email:tina.du@unisa.edu.au

Keywords: steel tube confined concrete; axial limit capacity; confined concrete; buckling of the steel shell; stabilized capacity;

Abstract: This paper presents an approach for the ultimate load analysis of steel tube confined concrete (STCC) columns. Based on the flexural behaviour of the steel shell the axial stabilized capacity of the column was deduced. A finite element analysis model and Matlab programs were developed to analyze the mechanisms of STCC columns under axial compression, in which both the geometric and material non-linearity were taken into account. The results show that both the predicted ultimate strength and load versus deformation curves demonstrate generally good agreements with the experimental data.

1. Introduction

Due to the restraint action of the steel tube to the core concrete, steel tube confined concrete is one kind of confined concrete, in which the compressive strength of the concrete is enhanced, whilst steel tube stability is increased. At present there are many studies on the limit capacity of STCC columns. The commonly used computing methods include the limiting equilibrium theory (Cai 2003), the unification material theory (Han 2007), the restraint concrete theory, and the double shears theory of unification strength. All of the above theories place reliance on the core concrete; however literature (Timoshenko 1936) reports that the steel tube undergoes buckling under the axial compression, which is a sign of rapid deduction in the flexure of the steel shell.

2. Computation model

2.1 Basic Assumptions

(1)The steel tube does not undergo partial loss of stabilization before the component achieves the stabilized-capacity, the paste between the steel tube and the core concrete are good and there is no relative slip and deformation between them;

(2) With an increasing load, the steel tube concrete section remains plane throughout, and the steel tube and the concrete cross-sectional areas remain constant;

(3)The longitudinal direction of the steel tube is divided into m half-waves (axial half wave numbers), while the circumference is divided into n half-waves (circle half wave numbers) when in flexure.

2.2 Numerical analysis of the steel tube behavior in flexure

When the STCC columns are under axial compression, the steel tube will be acted upon by axial and lateral pressure. The column shell (namely the steel tube) is able to maintain its cylindrical shape when the axial compression is small, however when it achieves some critical value, the cylindrical equilibrium shape may become unstable; therefore, failure in flexure begins to occur.

As shown in Fig. 1, u、v and w represent the small displacement of steel shell when flexure leaves the initial point along the x axis direction (longitudinal direction), the y axis direction (circle direction), and the z axis direction (radial direction), respectively. Three differential balanced equations were deduced by taking a shell element on the steel tube to determine the displacements.

$$\begin{cases} a^2\frac{\partial^2 u}{\partial x^2} + \frac{1+\mu}{2}a\frac{\partial^2 v}{\partial x\partial\theta} - \mu a\frac{\partial w}{\partial x} + a\varphi_1\left(\frac{\partial^2 v}{\partial x\partial\theta} - \frac{\partial w}{\partial x}\right) + \frac{1-\mu}{2}\frac{\partial^2 u}{\partial\theta^2} = 0 \\ \frac{1+\mu}{2}a\frac{\partial^2 u}{\partial x\partial\theta} + \frac{1-\mu}{2}a^2\frac{\partial^2 v}{\partial x^2} + \frac{\partial^2 v}{\partial\theta^2} - \frac{\partial w}{\partial\theta} + a\left[\frac{\partial^2 v}{\partial\theta^2} + \frac{\partial^3 w}{\partial\theta^3} + a^2\frac{\partial^3 w}{\partial x^2\partial\theta} + a^2(1-\mu)\frac{\partial^2 v}{\partial x^2}\right] - a^2\varphi_2\frac{\partial^2 v}{\partial x^2} = 0 \\ \mu a\frac{\partial u}{\partial x} + \frac{\partial v}{\partial\theta} - w - a\left[\frac{\partial^3 v}{\partial\theta^3} + (2-\mu)a^2\frac{\partial^3 v}{\partial x^2\partial\theta} + a^4\frac{\partial^4 w}{\partial x^4} + \frac{\partial^4 w}{\partial\theta^4} + 2a^2\frac{\partial^4 w}{\partial x^2\partial\theta^2} + \right] - \varphi_1\left(w + \frac{\partial^2 w}{\partial\theta^2}\right) - \varphi_2 a^2\frac{\partial^2 u}{\partial x^2} = 0 \end{cases} \tag{1}$$

where $\varphi_1 = \frac{qa(1-\mu^2)}{Eh}$, $\varphi_2 = -\frac{N_x(1-\mu^2)}{Eh}$.

Following published literature (Timoshenko 1936), E, μ, a and h are the elastic modulus, Poisson ratio, radius, and thickness of the steel tube, respectively, while q is lateral equal pressure (hydrostatic pressure) in the steel tube. Supposing both sides of the shell are the simple support, we get

$$\begin{cases} u = A\sin\left(\frac{n}{2}\theta\right)\cos\frac{m\pi x}{l} \\ v = B\cos(\frac{n}{2}\theta)\sin\frac{m\pi x}{l} \\ w = C\sin(\frac{n}{2}\theta)\sin\frac{m\pi x}{l} \end{cases} \tag{2}$$

Substituting Eq. (2) into Eq. (1) yields three uneven sub-linear equations which contain A, B and C. After equating the determinant of the above equations equal to zero, the marginal value equation is able to be solved, and is in the following form through the simplification;

$$C_1 + C_2\frac{h^2}{12a^2} = C_3\varphi_1 + C_4\varphi_2 \tag{3}$$

Where $C_1 = (1-\mu^2)\lambda^4$, $C_2 = \left(\lambda^2 + \frac{n^2}{4}\right)^4 - 2\left[\mu\lambda^6 + \frac{3\lambda^4 n^2}{4} + \frac{(4-\mu)\lambda^2 n^4}{16} + \frac{n^6}{64}\right] + \frac{(2-\mu)\lambda^2 n^2}{2} + \frac{n^4}{16}$,

$C_3 = \frac{n^2}{4}\left(\lambda^2 + \frac{n^2}{4}\right)^2 - \left(\frac{3n^2\lambda^2}{4} + \frac{n^4}{16}\right)$, $C_4 = \lambda^2\left(\lambda^2 + \frac{n^2}{4}\right)^2 + \frac{n^2\lambda^2}{4}$, and $\lambda = \frac{m\pi a}{l}$.

According to experimental investigations, researchers (Richart 1928) believe that lateral equal pressure p (hydrostatic pressure) maintains a linear relationship to the ultimate concrete strength f_{cc}.

$$f_{cc} = f_c + k * p \tag{4}$$

Where f_c represents the compressive strength of the concrete without any lateral pressure, and k is a coefficient decided by the experiments which would take the value of 4 generally. The rearrangement of Eq. (4) yields;

$$p = \frac{f_{cc} - f_c}{k} \tag{5}$$

The force balance as depicted in Fig. 2 yield;

$$N_u = A_c * f_{cc} + A_t * \sigma_{tz} = A_c * f_{cc} + N_x \tag{6}$$
$$f_{cc} = (N_u - N_x)/A_c \tag{7}$$

Based on the comparisons between fifteen experimental results (Cai 2003, Han 2007), literature (Chen 2005) presents the limit capacity of the STCC column:

$$N_u = A_c * f_c + 2A_t * f_{yt} \tag{8}$$

Substituting Eq. (8) into (7) yields;

$$f_{cc} = (A_c * f_c + 2A_t * f_{yt} - N_x)/A_c \tag{9}$$

Substitution of Eq. (9) into (5);

$$p = \left[\frac{A_c*f_c+2A_t*f_{yt}-N_x}{A_c} - f_c\right]/k = (2A_t * f_{yt} - N_x)/A_c k \tag{10}$$

Followed by substitution of Eq. (10) into (3);

$$N_x = \frac{(C_1+C_2\alpha)-2K_1 A_s f_{yt}}{K_2 - K_1} \tag{11}$$

where $K_1 = \frac{C_3 a(1-\mu^2)}{4A_c E_s t}$ and $K_2 = \frac{-C_4(1-\mu^2)}{E_s t}$. Finally substituting Eq. (4), (10) and (11) into (6), we are able to derive Eq. (12), which is the governing axial stabilized capacity of a STCC column

$$N_{stabilized} = N_u = A_c * f_{cc} + N_x = \frac{(C_1+C_2\alpha)-2K_1 A_s f_{yt}}{K_2-K_1} + (f_c + 4\frac{2A_t*f_{yt}-\frac{(C_1+C_2\alpha)-2K_1 A_s f_{yt}}{K_2-K_1}}{A_c k})A_c \tag{12}$$

3. Solution patterns and computer results
From Eq. (12) we find that the axial capacity of the STCC column is reliant on the value of the axial half-wave number m and circle half-wave number n. In fact, m and n are the only two independent variables in Eq. (12). Hence, deducing the axial stabilized capacity of an STCC column, by accounting for the flexure of the steel shell required the process of determining reasonable value of m and n.

3.1 Method A: Global search of the minimum value
Making independent variables m and n equal to 1,2,3,4 and so on, we find the minimum value, namely $N_{stabilized}$ by implementing a Matlab program.

3.2 Method B: Theory analytic with the pattern
As published in literature (Timoshenko 1936), in the case of the symmetrical flexure of the column shell under even axial compressive;

$$\frac{m\pi}{L} = \sqrt[4]{\frac{Et}{a^2 D}} \tag{13}$$

where D represents the flexible rigidity of the shell. Whilst, Timoshenko (1936) believes the flexure of the column shell result in small waves of lengths that are the same in the axial and radial directions; $\lambda_m = \lambda_n = \frac{L}{m}$, which yields;

$$n = \frac{2m\pi a}{L} \tag{14}$$

Consequently, depending on Eq. (13) and (14), we obtain m and n based on the geometric and physical parameters of the shell.

4. Discussion on method A and method B
By using Method A, the smallest $N(m,n)$ results in m equaling 1 or 2 (Table 3), but it is evident from Table 2 that nearly half of the m values are acceptable in the matrix, notably when $m>n$, $N(m,n) \approx N_{stabilized}$. However, m, which is derived out according to the Eq. (13) by employing Method B, implies that after achieving a particular value, the axial half-wave m may not be the integer. This question can also be interpreted as that after achieving a certain value; the modification of the constraint conditions at column ends result in little influence to the limit capacity of columns. Since we did not consider the initial flaw of the steel tube, most predicted values are larger than the

3

experimental data, despite implementing Method A or Method B. Although both Method A and Method B theoretically reasonable, the calculation methods of deriving m, n values are vastly different between the two methods. The reason may be that all of the steel shells have the initial flaw (the major factor is local sudden curvature changes of the steel tube), but the degree of initial flaw is not at the same level. While the more serious of the initial flaw of the steel tube has its failure shape show less agreement to Method B, while it would be more agreed to with Method A. The relationships of initial flaw and failure Methods can be tested by program *Abaqus* or *Ansys*.

5. Conclusions

1. From thin shell to thick shell (t/D=0.01~0.1), ordinary concrete to high intensity concrete, they all can be unified in the governing axial stabilized capacity of the STCC column Eq. (12). As the assumption (1) considering perfectly intact between the steel tube and confined concrete, it leads that the theoretical model always predict the axial strength of concrete-filled-steel-tube columns on the high side (i.e. overestimating the actual strength – see Table 3);

2. The buckling stress of shell approach to $0.8f_{yt}$ which agrees well with "Method C: Von Mises model" in literature (Chen 2005);

3. Both Method A and Method B are certain theoretically rationality, however the destructive patterns are mainly depended on the initial flaw of the steel tube.

6. TABLES AND FIGURES

Table 1. Parameters of some experimental specimens (Cai 2003).

Specimens	D×t×L (mm)	E_s (N/mm^2)	f_s (N/mm^2)	f_{cu} (N/mm^2)
No. 1	96×5×400		410	48.4
No. 2	204×2×840		235	35
No. 3	273×8×1100		307	49
No. 4	96×5×450		410	35
No. 5	108×4×324	$2×10^5$	338.9	35.7
No. 6				35
No. 7	121×12×500		294	12.8
No. 8				49
No. 9				16.5

Table 2. $N_{stabilized}$ (×10^{6}N) calculated by the different value of m and n of test Specimen 1.

	n=1	2	3	4	5	6	7	8	9	10	11	12
m=1	2.03	1.47	1.38	1.41	1.60	2.01	2.73	3.85	5.43	7.54	10.21	35.4
2	2.60	1.67	1.46	1.42	1.45	1.56	1.78	2.12	2.63	3.34	4.30	5.54
3	2.40	1.77	1.53	1.45	1.44	1.48	1.58	1.75	1.99	2.34	2.81	3.42
4	2.10	1.76	1.566	1.47	1.45	1.46	1.52	1.61	1.76	1.97	2.25	2.61
5	1.89	1.71	1.57	1.49	1.46	1.46	1.49	1.56	1.65	1.79	1.98	2.23
6	1.75	1.65	1.56	1.50	1.47	1.46	1.48	1.53	1.60	1.70	1.84	2.01
7	1.66	1.60	1.54	1.50	1.47	1.47	1.48	1.51	1.57	1.65	1.75	1.89
8	1.61	1.57	1.53	1.49	1.47	1.47	1.48	1.51	1.55	1.61	1.70	1.81
9	1.56	1.54	1.51	1.49	1.48	1.47	1.48	1.50	1.54	1.59	1.66	1.76
10	1.53	1.52	1.50	1.49	1.48	1.48	1.48	1.50	1.54	1.58	1.64	1.72

Table 3 Comparison of the predicted values and experimental data of those specimens in Table 1.

Specimens	Experimental value (KN)	Method A				Method B			
		Predicted Value(KN)	m	n	Relative Error e_r	Predicted Value(KN)	m	n	e_r
No. 1	1130	1412	1	4	-24	1205	16	11	-6.6

No. 2	1295	1284	1	8	0.84	1218	35	26	5.9
No. 3	5200	5782	1	4	-11	4992	20	15	4
No. 4	1105	1363	2	4	-23	1153	18	11	-4.3
No. 5	1000	1091	1	4	-9.1	943	13	13	5.7
No. 6	2500	2844	1	2	-13	2504	12	8	-0.16
No. 7	2300	2734	1	2	-18	2394	12	8	-4.1
No. 8	2600	2913	1	2	-12	2573	12	8	1.04
No. 9	2746	2752	1	2	-0.22	2412	12	8	12.2
Average e_r					-12.16				1.52
Standard Deviation					8.76				6.03

Relative error e_r= (Experimental value - Predicted value)/Experimental value $\times 100\%$
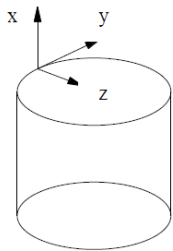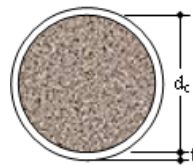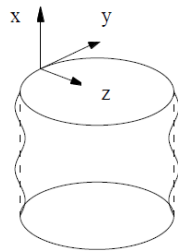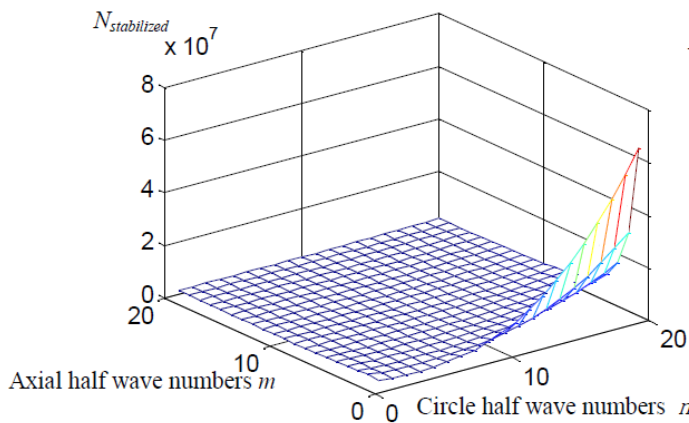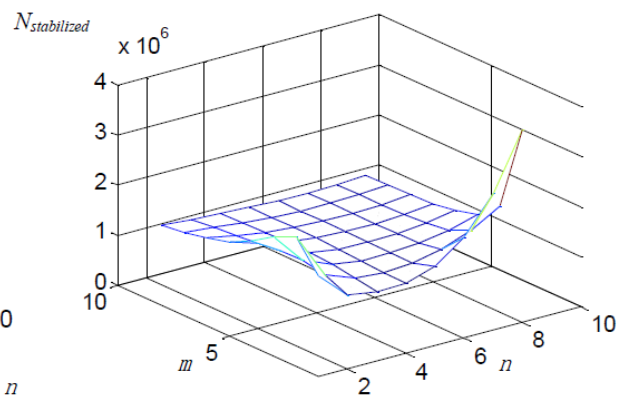

Fig.1. Small displacement of steel shell
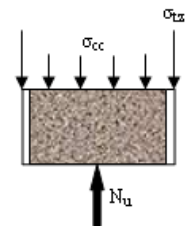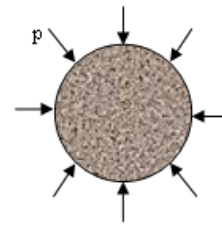
Fig. 2. The bearing stress of the steel tube and confined concrete

(a) (b)

Fig.3. $N_{stabilized}$ inferred from the different value of m and n of test sample 1

7. References

[1]Cai, S.H. (2003) Steel Tube Confined Concrete Structures. People's Translation Press.

[2]Chen, Y.J. (2005) Constitutive Model and Bearing Capacity of Confined Steel Reinforced Concrete Columns with Circular Steel Tube. [Masters Thesis]. Nanjing, China: Southeast University.

[3]Han, L.H. (2007) Concrete-filled steel tubular structures theory and practice. Beijing, China: Science Press.

[4]Richart, F.E. (1928) A study of the failure of concrete under combined compressive stresses, University of Illinois Bulletin, Vol. 26, No. 12.

[5]Timoshenko, S. (1936) Theory of Elastic Stability. McGraw-Hill Book Company Inc.